in bimolecular electron transfers has been difficult to obtain.[37]

Acknowledgment. We thank M. Chou for assistance with some of the emission measurements. This work was performed at Brookhaven National Laboratory under contract DE-AC02-76CH00016 with the U.S. Department of Energy and supported by its Division of Chemical Sciences, Office of Basic Energy Sciences.

(37) Creutz, C.; Sutin, N. *J. Am. Chem. Soc.* **1977**, *99*, 241.

Registry No. $Ru(bpy)_3^{2+}$, 15158-62-0; $Ru(bpy)_3^{3+}$, 18955-01-6; $Ru(4,7\text{-}(CH_3)_2phen)_3^{2+}$, 24414-00-4; $Ru(4,7\text{-}(CH_3)_2phen)_3^{3+}$, 79747-03-8; $Os(terpy)_2^{2+}$, 85452-91-1; $Os(terpy)_2^{3+}$, 100815-62-1; $Co(bpy)_3^{+}$, 47780-35-8; $Co(4,4'\text{-}(CH_3)_2bpy)_3^{+}$, 47837-97-8; $Co(terpy)_2^{3+}$, 18308-16-2; $Co(terpy)_2^{+}$, 47779-83-9.

Solvation Structure of a Sodium Chloride Ion Pair in Water

Alan C. Belch,*† Max Berkowitz,*† and J. A. McCammon*‡

Contribution from the Departments of Chemistry, University of North Carolina, Chapel Hill, North Carolina 27514, and the University of Houston, Houston, Texas 77004.
Received June 13, 1985

Abstract: Changes in the equilibrium solvation structure associated with the separation of a Na^+Cl^- ion pair in water have been examined with use of computer simulation. At all separations, the Na^+ attempts to maintain an octahedral shell of nearest neighbors. This shell is comprised of five waters and the chloride in the stable contact ion pair. When the ions are separated slightly, the five waters rotate, weakening their hydrogen bonding with the second shell waters and producing a distorted octahedron. Those waters which rotate toward the chloride assume "bridging" orientations characterized by favorable electrostatic interactions with both ions. Further separation leads to replacement of the chloride by a sixth water molecule and formation of a stable solvent-separated ion pair in which strong hydrogen bonds are again formed between the first and second shells near Na^+. More subtle changes in structure and interactions occur farther from the Na^+ and around the Cl^-; these changes are noticeable up to about 7 Å from each ion.

I. Introduction

The association of oppositely charged ions is an important step in many chemical reactions and in the formation and activity of many biological molecules.[1] Many rapid ionic reactions in solution apparently have very small barriers and therefore are diffusion controlled. The influence of strong electrostatic forces on the diffusive approach rate of ions was successfully studied by Onsager[2] and Debye[3] using continuum theories. Later, it became apparent that for ionic reactions with high barriers a more detailed level of microscopic description is necessary. Thus the idea of a solvent-separated ion pair $A^+||B^-$ separated by a barrier from the contact ion pair A^+B^- was introduced by Fuoss[4] and Winstein.[5] The clarification of the role played by solvent in the process of ion pair interconversion from solvent-separated into close contact configurations is an important step in our understanding of chemical reactivity in solutions.

Because of the importance of water as a solvent, we concentrate on properties of ionic pairs in aqueous solutions. Recently we obtained the form of the potential of mean force for a sodium chloride ion pair in water using molecular dynamics computer simulation.[6] Distinct minima in the free energy of the system were found for contact and solvent separated ion geometries at 25 °C. In the present paper we report a detailed analysis of the solvation structure of the same system as a function of ion–ion distance. The method used in this work is outlined in section II. In section III, we discuss the results on structural and energetic changes in water around the ion pair. Section IV presents the concluding remarks.

II. Method

Molecular dynamics simulations were carried out on a system of 295 TIPS2 water molecules and a single Na^+Cl^- ion pair. The ions were held at fixed separation distances of 2.7, 3.7, 5.0, and 5.6 Å in successive simulations. These distances were selected from the minima and maxima of the potential of mean force calculated by Berkowitz et al.[6] The value 2.7 Å represents the contact pair distance, 5.0 Å and 5.6 Å are solvent separated distances, and 3.7 Å is the distance at a maximum of the potential of mean force and therefore represents a transition-state region. The box for the simulation was rectangular; lengths of the sides were 18.6, 18.6, and 25.4 Å. The long dimension was chosen to be along the ion-pair separation vector so as to minimize artifacts associated with the use of periodic boundary conditions.

Table I. TIPS2 Parameters for Water, Na^+, and Cl^-

site	q(electrons)	$10^{-3}A^2$, kcal Å^{12}/mol	C^2, kcal Å^6/mol
O in H_2O	0.000	695	600
M in H_2O	−1.070	0	0
H in H_2O	0.535	0	0
Na^+	1.0	14	300
Cl^-	−1.0	26 000	3500

The potentials employed were the TIPS2 potential for the water–water interaction and similar TIPS2-like potentials for the ion–ion and ion–water interactions.[7] These potentials are of the form shown in eq 1. The

$$U_{mn} = \sum_{i \in m} \sum_{j \in n} \left(\frac{q_i q_j e^2}{r_{ij}} + \frac{A_i A_j}{r_{ij}^{12}} - \frac{C_i C_j}{r_{ij}^{6}} \right) \quad (1)$$

parameters for the potentials are shown in Table I. The interactions were truncated at 8.5 Å and polarization effects were not included. These potentials were shown to give a reliable representation of a solvation structure in single ion hydration.[7]

The dynamics were carried out with use of the Verlet algorithm with SHAKE[8] on a VAX 11/780. The time step was 4 fs and each configu-

† University of North Carolina.
‡ University of Houston.

(1) Lowry, T. H.; Richardson, K. S. "Mechanism and Theory in Organic Chemistry"; 2nd ed.; Harper and Row: New York, 1981.
(2) Onsager, L. *Phys. Rev.* **1938**, *54*, 554.
(3) Debye, P. *Trans. Electrochem. Soc.* **1942**, *82*, 265.
(4) Sadek, H.; Fuoss, R. *J. Am. Chem. Soc.* **1954**, *76*, 5897.
(5) Winstein, S.; Clippinger, E.; Fainberg, A. H.; Robinson, G. C. *J. Am. Chem. Soc.* **1954**, *76*, 2597.
(6) Berkowitz, M.; Karim, O. A.; McCammon, J. A.; Rossky, P. J. *Chem. Phys. Lett.* **1984**, *105*, 577.
(7) Jorgensen, W. L. *J. Chem. Phys.* **1982**, *77*, 4156. Jorgensen, W. L.; Madura, J. W.; Impey, R. W.; Klein, M. L. *J. Chem. Phys.* **1983**, *79*, 926. Jorgensen, W. L.; Chandrasekhar, J. *J. Chem. Phys.* **1982**, *77*, 5080.

0002-7863/86/1508-1755$01.50/0

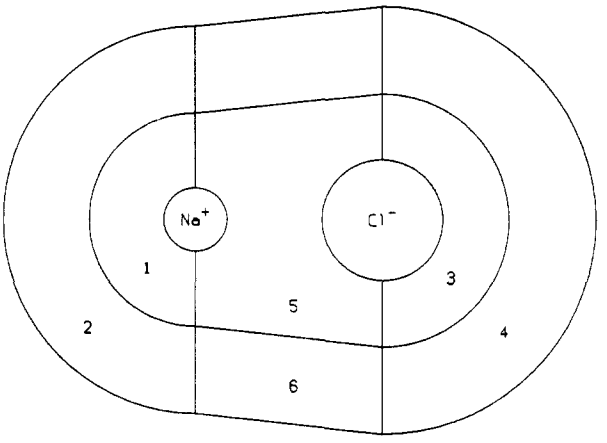

Figure 1. Defined regions around the Na^+Cl^- ion pair.

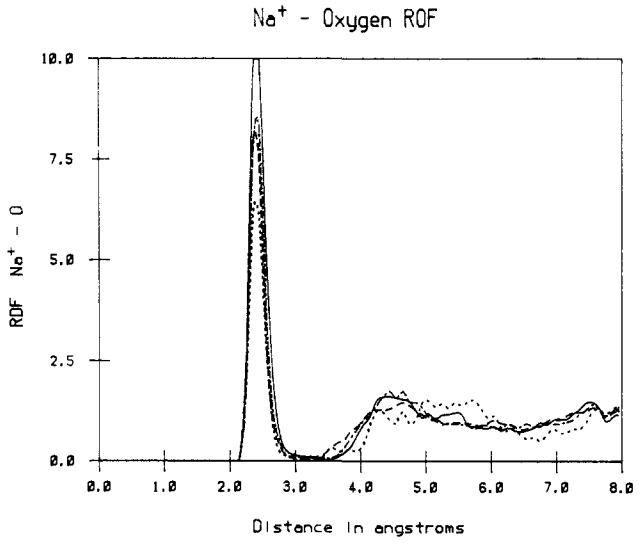

Figure 2. The Na^+–oxygen radial distribution function for ions separated by 2.7, 3.7, 5.0, and 5.6 Å. The solid line is for 2.7 Å, the dotted line for 3.7 Å, the dashed line for 5.0 Å, and the dot-dashed line for 5.6 Å.

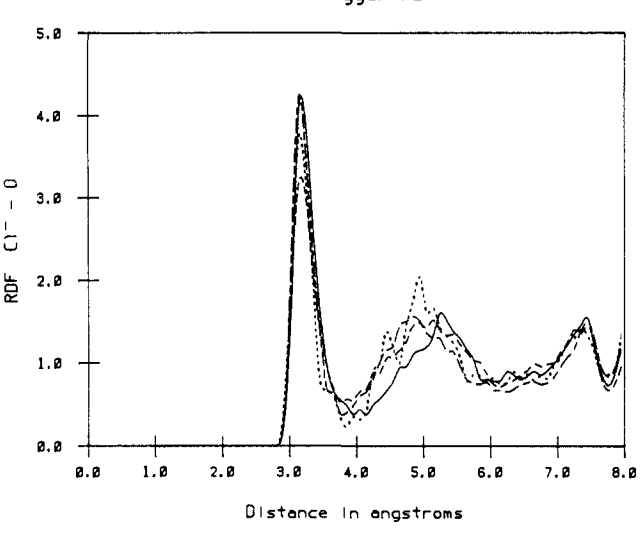

Figure 3. The Cl^-–oxygen radial distribution function for ions separated by 2.7, 3.7, 5.0, and 5.6 Å. Line types are described in Figure 2.

ration was saved after an initial 10-ps equilibration. The four runs were each of 20-ps duration. The mean temperature in each run was 297.2 K. Although not molecular dynamics in the truest sense, the method of fixing the ions allows for a representative sampling of water structure phase space.

(8) Verlet, L. *Phys. Rev.* **1967**, *159*, 98. Ryckaert, J. P.; Ciccotti, G.; Berendsen, H. J. C. *J. Comput. Phys.* **1977**, *23*, 327.

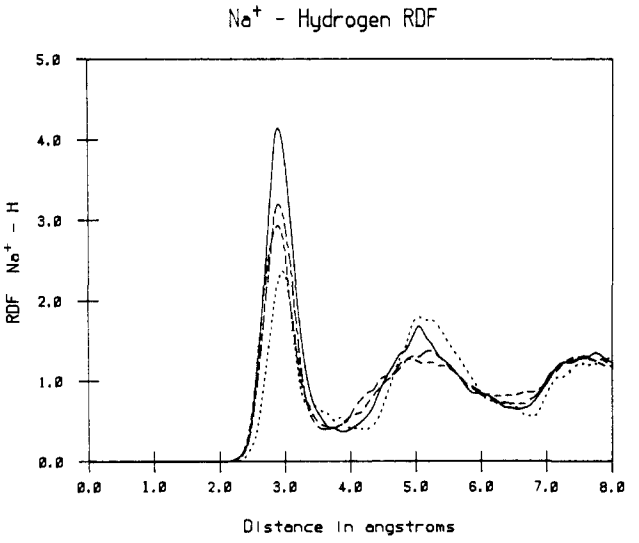

Figure 4. The Na^+–hydrogen radial distribution function for ions separated by 2.7, 3.7, 5.0, and 5.6 Å. Line types are described in Figure 2.

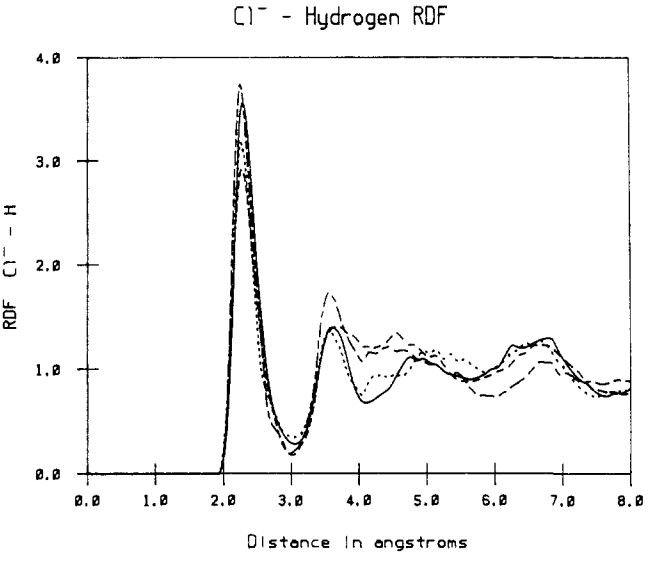

Figure 5. The Cl^-–hydrogen radial distribution function for ions separated by 2.7, 3.7, 5.0, and 5.6 Å. Line types are described in Figure 2.

III. Results and Discussion

The structure of water around the ion pair is a function of the relative positions of the water molecules with respect to both ions. In order to differentiate between different environments, we defined seven regions around the ion pair. Bisecting planes, perpendicular to the ion separation vector and passing through the centers of the ions, divide the system into three volumes. The end volumes can be considered mainly under the influence of the closest individual ion and can be subdivided into two hemispheres whose boundaries are determined by the ion–oxygen radial distribution functions (rdf). The inner volume can be divided into two cylindrical regions joining the hemisphere boundaries. The remaining volume of the system may be considered bulk. Figure 1 graphically represents these regions with labels. Regions 1 and 3 are called the first external hydration shell (FEHS). Regions 2 and 4 are called the second external hydration shell (SEHS). Regions 5 and 6 are called the first and second internal hydration shells respectively (FIHS and SIHS). Region 7 is the bulk water.

The radial distribution functions between the ions and water were calculated for the external volumes of water discussed above. The ion–oxygen and ion–hydrogen rdfs are presented in Figures 2–5. The integrated intensities and populations of the internal volumes are presented in Table II. The peak locations compare

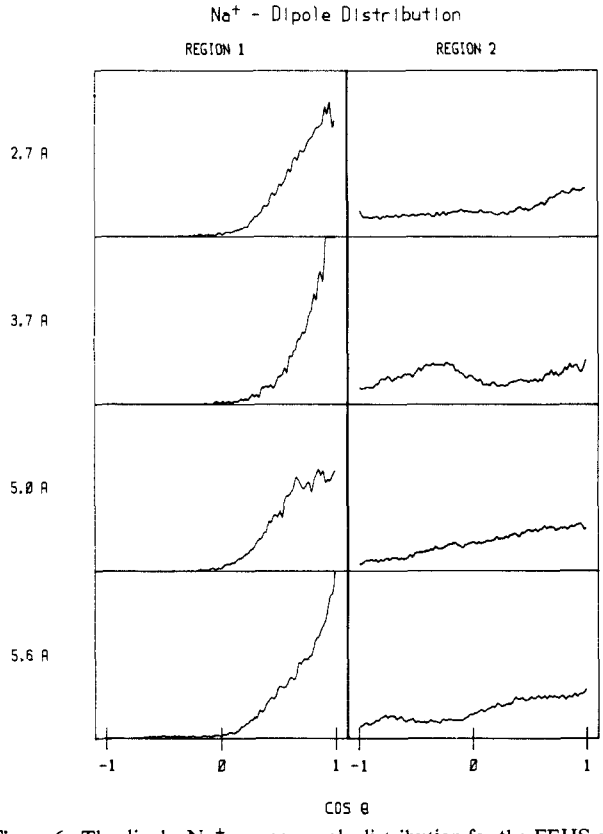

Figure 6. The dipole–Na^+–oxygen angle distribution for the FEHS and SEHS for ions separated by 2.7, 3.7, 5.0, and 5.6 Å.

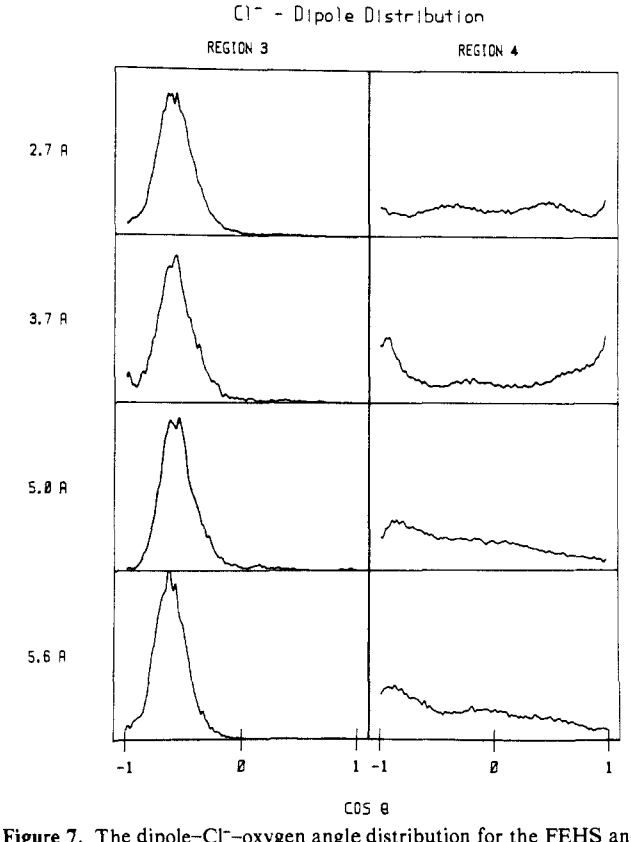

Figure 7. The dipole–Cl^-–oxygen angle distribution for the FEHS and SEHS for ions separated by 2.7, 3.7, 5.0, and 5.6 Å.

favorably with those obtained by Impey et al.[9] and Jorgensen et al.[7] From the radial distribution functions, it is clear that the

(9) Impey, R. W.; Madden, P. A.; McDonald, I. R. *J. Phys. Chem.* **1977**, *87*, 5071.

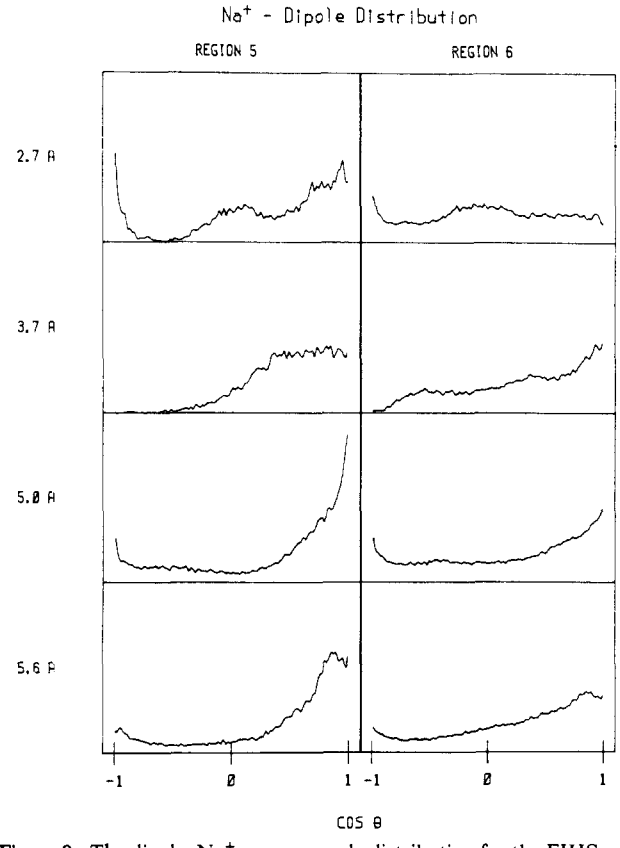

Figure 8. The dipole–Na^+–oxygen angle distribution for the FIHS and SIHS for ions separated by 2.7, 3.7, 5.0, and 5.6 Å.

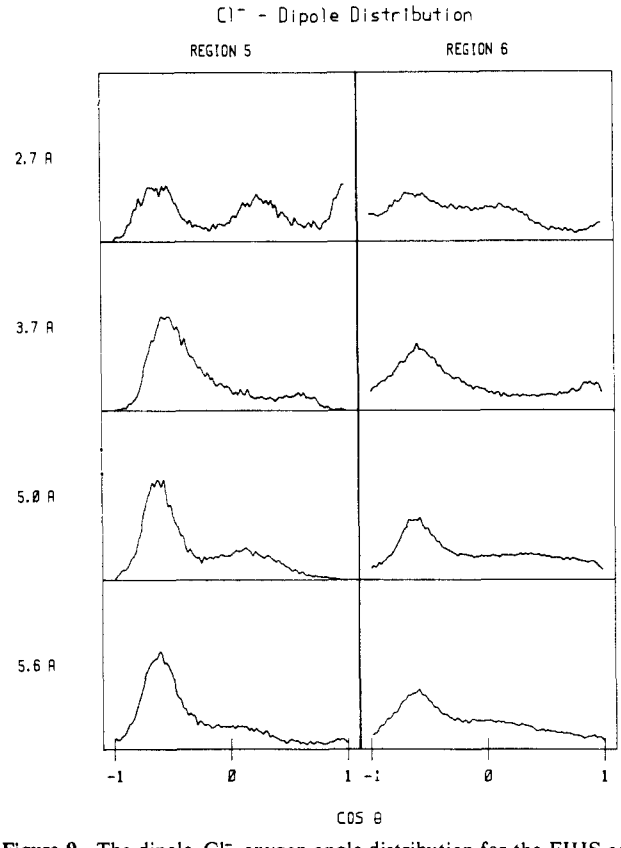

Figure 9. The dipole–Cl^-–oxygen angle distribution for the FIHS and SIHS for ions separated by 2.7, 3.7, 5.0, and 5.6 Å.

solvent near Na^+ is relatively highly ordered in the stable ion pair configurations (i.e., for the 2.7- and 5.0-Å separations). In the transition-state configurations, there is a decreased population corresponding to the first peak and the second peak is relatively

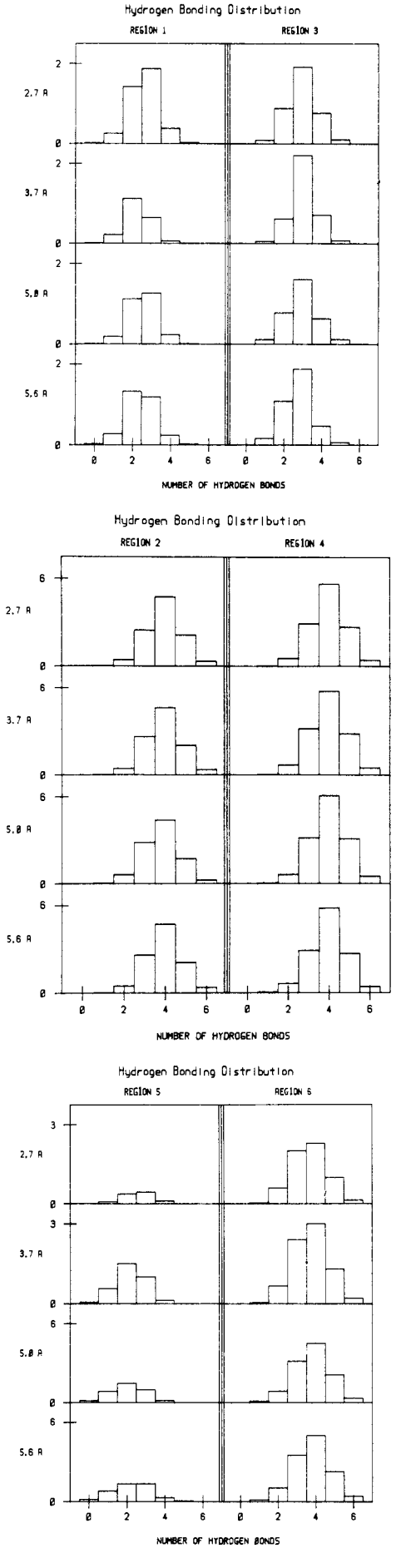

Figure 10. Hydrogen bonding distributions.

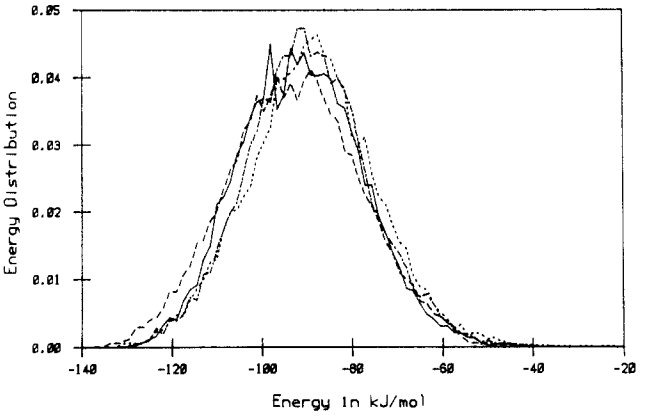

Figure 11. Interaction energy distribution, region 1.

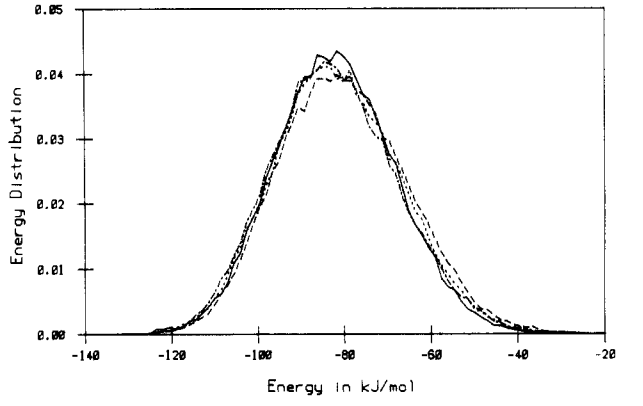

Figure 12. Interaction energy distribution, region 2.

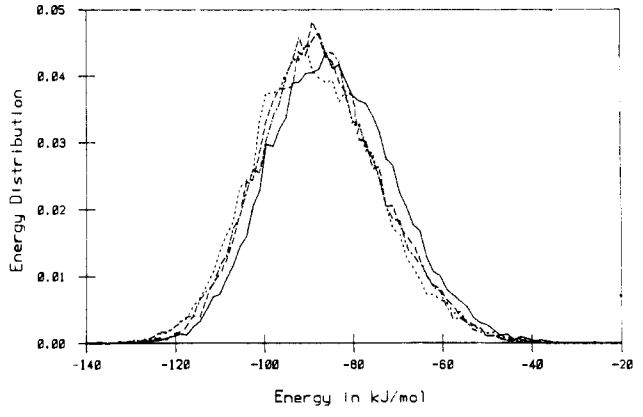

Figure 13. Interaction energy distribution, region 3.

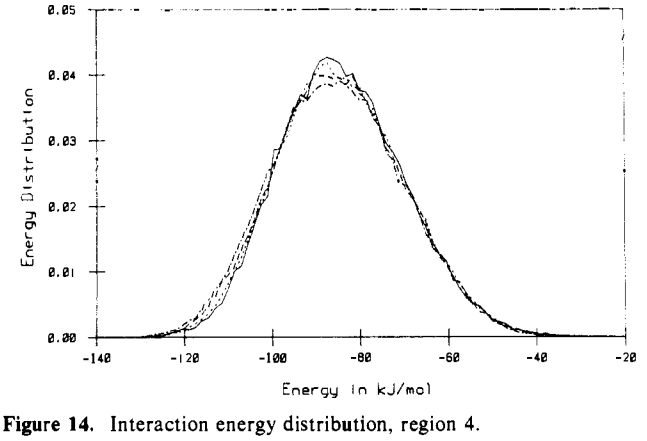

Figure 14. Interaction energy distribution, region 4.

diffuse. Smaller differences occur near Cl^-, although the second-shell oxygens are drawn closer to Cl^- in the noncontact configurations.

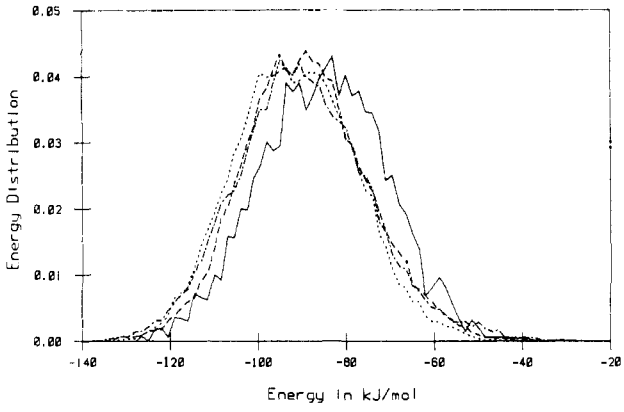

Figure 15. Interaction energy distribution, region 5.

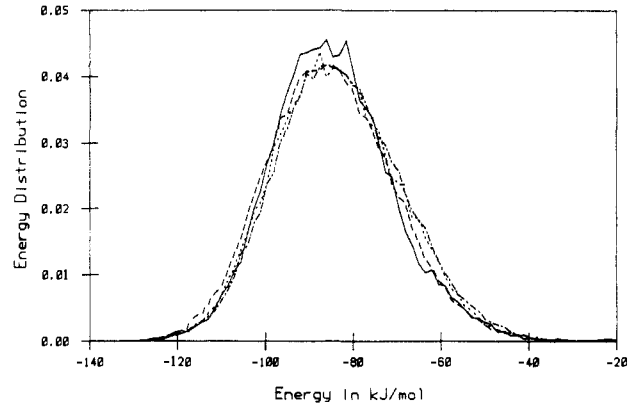

Figure 16. Interaction energy distribution, region 6.

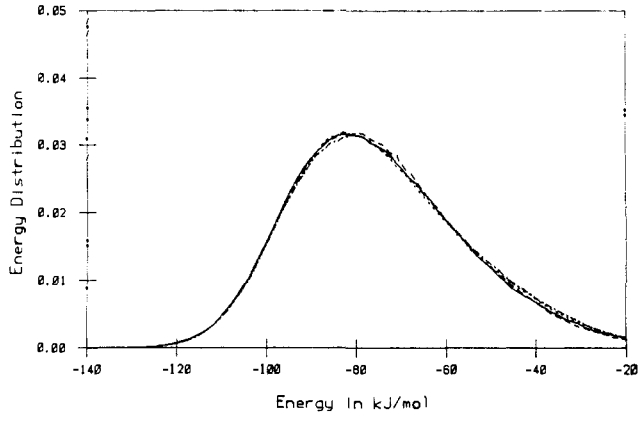

Figure 17. Interaction energy distribution, bulk water.

The radial distribution functions do not provide adequate structural information by themselves and must be supplemented by angular distributions as well. The angles of interest are those between the water dipoles (i.e., the direction from O to the centroid of the H's) and the vectors from the ions to the oxygens. These angles are similar to those checked by Impey et al.[9] Our angle between the O–Cl^- vector and the dipole differs from the previously mentioned work by a phase shift of π. The results of the angular distributions by region are shown in Figures 6–9.

The angular distribution difference between the stable ion separation distances and the "transition" distance is quite striking for the Na^+–H_2O interactions. The most probable angle for the contact pair is 25°, indicating that the hydrogens and one lone pair should typically be available for hydrogen bonding. At 3.7 Å ion separation, the water dipoles point more directly away from the ion, thus reducing the available hydrogen-bonding sites to two. It should also be noted that this alignment perturbs the SEHS with a relatively flat distribution becoming bi-modal. This indicates a long-range structural effect for the transition state. At 5.0-Å separation, the Na^+–H_2O angles relax somewhat from the highly ordered situation in the transition region, so that more hydrogen-bonding possibilities are again available.

Table II. Average Population per Region

ion separation, Å	region 1	2	3	4	5	6
2.7	3.97	10.23	3.77	12.03	1.64 (1.00)[a]	8.54 (1.00)
3.7	2.05	10.39	3.42	13.08	4.57 (2.04)	12.18 (1.04)
5.0	2.82	9.86	3.29	13.59	5.18 (1.71)	16.07 (1.02)
5.6	2.99	10.29	3.63	12.56	5.49 (1.62)	18.61 (1.05)

[a] Note: The value reported in parentheses for regions 5 and 6 are reported on a per volume basis.

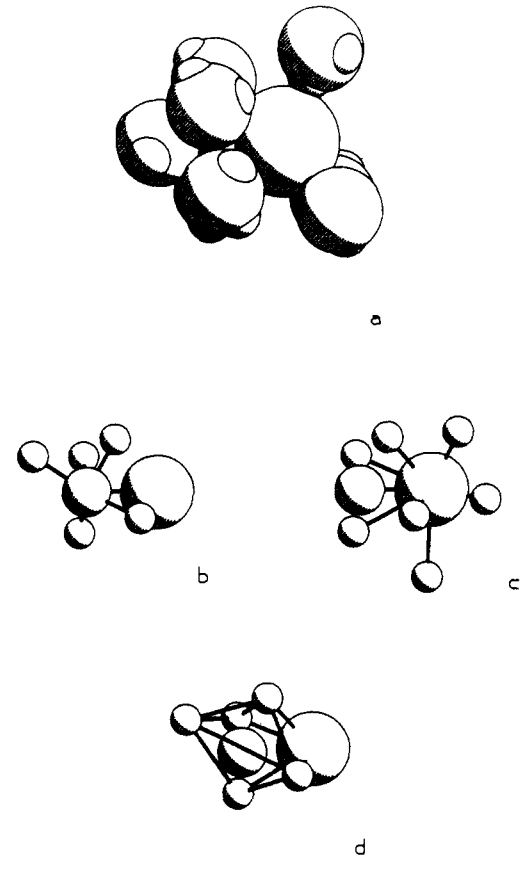

Figure 18. Structure of first common hydration shell around ions separated by 2.7 Å. (a) Instantaneous configuration. (b) First shell around Na^+, oxygens, and Cl^- only, diffusionally averaged structure. (c) First shell around Cl^-, oxygens, and Na^+ only, diffusionally averaged structure. (d) Diffusionally averaged structure showing octahedron around Na^+. Bonds are shown only for space perspective viewing.

The dipole angle distribution in region 3 for Cl^- shows no significant change through the transition state. The most probable angle is 140° which is suggestive of a water structure which has a hydrogen pointing toward the chlorine. In region 4, some structure is apparent at 3.7-Å separation; the two classes of waters with $\theta \approx 0°$ or $\theta \approx 155°$ correspond to favorable orientations for hydrogen bonding with first shell waters.

The distribution functions in the inner volume reflect the competition between the orienting fields of the two ions. For the 2.7-Å separation, there appear to be two distinct classes of water molecules in region 5. Those that are closer to Na^+ tend to have their dipoles pointing away from that ion, producing the peaks near $\cos\theta = 1$ in Figure 8 and near $\cos\theta = 0.3$ in Figure 9. Those that are closer to Cl^- tend to have their hydrogens pointing toward that ion, producing peaks near $\cos\theta = -1$ and 0 in Figure 8 and near $\cos\theta = -0.7$ in Figure 9. Display of representative molecular

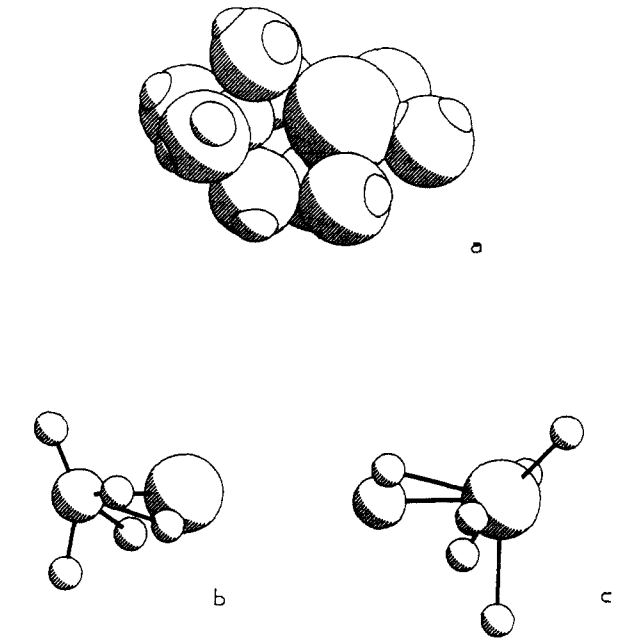

Figure 19. Structure of first common hydration shell around ions separated by 3.7 Å. (a) Instantaneous configuration. (b) First shell around Na^+, oxygens, and Cl^- only, diffusionally averaged structure. (c) First shell around Cl^-, oxygens, and Na^+ only, diffusionally averaged structure. Bonds are shown only for space perspective viewing.

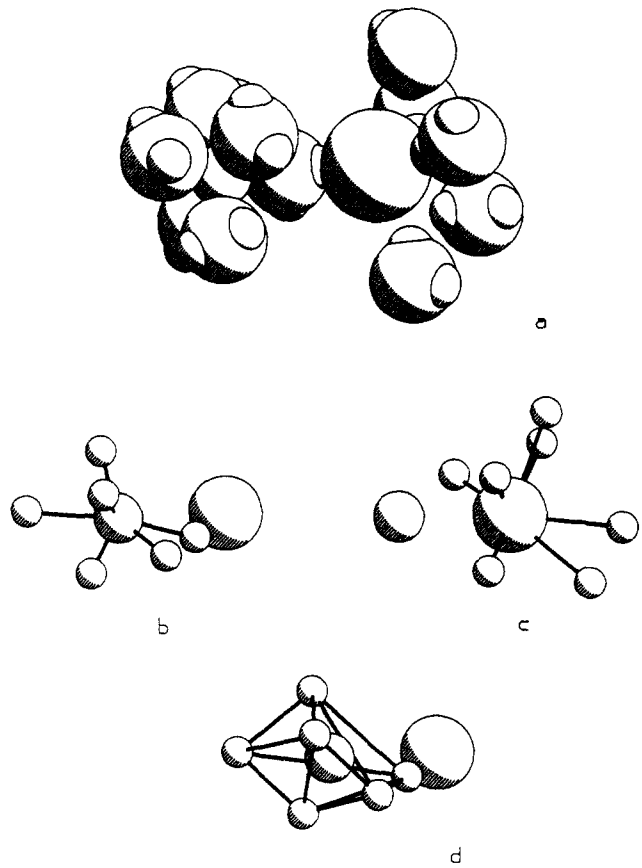

Figure 20. Structure of first common hydration shell around ions separated by 5.0 Å. (a) Instantaneous configuration. (b) First shell around Na^+, oxygens, and Cl^- only, diffusionally averaged structure. (c) First shell around Cl^-, oxygens, and Na^+ only, diffusionally averaged structure. (d) Diffusionally averaged structure showing octahedron around Na^+. Bonds are shown only for space perspective viewing.

structures confirms these trends, as will be seen below. For the larger separations (3.7, 5.0, and 5.6 Å), the water molecules in region 5 are mostly of a single "bridging" class. These waters are

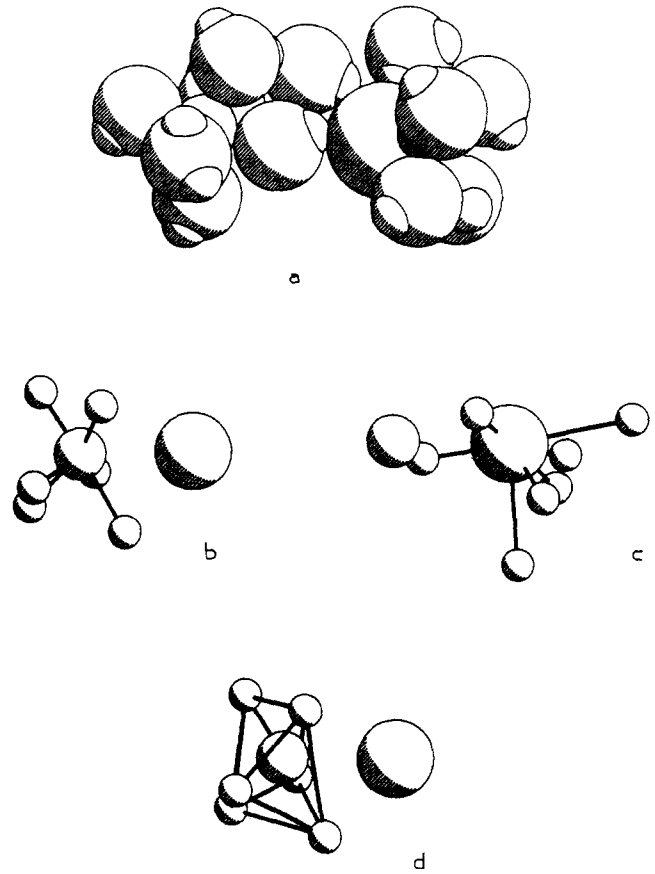

Figure 21. Structure of first common hydration shell around ions separated by 5.6 Å. (a) Instantaneous configuration. (b) First shell around Na^+, oxygens, and Cl^- only, diffusionally averaged structure. (c) First shell around Cl^-, oxygens, and Na^+ only, diffusionally averaged structure. (d) Diffusionally averaged structure showing octahedron and Na^+. Bonds are shown only for space perspective viewing.

Table III. Average Number of Hydrogen Bonds per Molecule per Region

	ion separation in Å			
region	2.7	3.7	5.0	5.6
1	2.62	2.27	2.56	2.46
2	3.95	3.94	3.80	3.93
3	2.98	3.04	2.96	2.78
4	3.96	3.94	3.98	3.94
5	2.56	2.18	2.05	2.24
6	3.67	3.72	3.79	3.78

located more equidistantly from the two ions and can simultaneously satisfy the orientational requirements of each ion; i.e., the waters tend to have their dipoles pointing away from Na^+ and to have a hydrogen pointing toward Cl^-. The distribution at 2.7 Å is limited by the statistics of the number of waters which interact. The distribution for region 6 shows that the environment of interaction extends radially more than 3.2 Å from the ion pair separation vector. This suggests a rugby ball shaped interaction region about the ion pair in infinite dilution, similar to that found in earlier cluster calculations by Clementi et al.[10]

The hydrogen bond distributions presented in Figure 10 were calculated with use of an energetic hydrogen bond definition of −2.5 kcal/mol. In region 1, the solvent hydrogen bonding is relatively weak in the transition-state region (3.7 Å); this is consistent with the increased dipolar alignment seen in Figure 6 and discussed above. The decreased hydrogen bonding to second-shell waters may account for the diffuseness of that shell in the radial distribution function (Figure 2). In region 3, on the

(10) Clementi, E.; Barsotti, R.; Fromni, J.; Watts, R. O. *Theor. Chim. Acta (Berlin)* **1976**, *43*, 101.

other hand, there tends to be a slight increase in hydrogen bonding in the transition-state region; this is also consistent with the dipolar alignment noted for region 4 in Figure 7. In region 5, the number of hydrogen bonds increases significantly as the ions are separated from the contact to the transition-state region; this is primarily due to the entry of solvent into this expanding volume, although there is a slight decrease in the number of hydrogen bonds per molecule (see Table III). The number of hydrogen bonds in region 5 remains fairly constant with further separation of the ions.

The pair interaction energy distributions for waters in each region were calculated and are presented in Figures 11–17. There is a 10–15-kJ/mol stabilization for the waters in region 1 over the bulk region at the equilibrium distance configurations. This stabilization is only about 5 kJ/mol for the transition-state configurations. A 5–10-kJ/mol stabilization occurs in region 3 with no difference between the equilibrium and transition-state configurations. Regions 2, 4, and 6 have a 0–5-kJ/mol stabilization with very similar distributions. Region 5 shows a bimodal energy distribution. This may be indicative of the different situations where the water attempts to either align its dipole with the Na^+ or a hydrogen with the Cl^-.

It is commonly assumed that Na^+ in water maintains an octahedral first solvation shell. The situation for Cl^- is less clear—some experiments place the average hydration number at six, while molecular dynamics simulations suggest seven. A study of the first common hydration shell (regions 1, 3, and 5) was carried out in order to ascertain the structure around the ion pair at infinite dilution. Two types of pictures can be generated. Instantaneous pictures give the most accurate geometries, but any one such picture cannot be fully representative of the sampled configurations. Pictures averaged over times on the order of 1 ps show the most probable orientations of possible solvation "cages". Earlier studies of water show that time-averaged configurations, with the appropriate time scale chosen, can give clear pictures of quasi-static structure.[11]

Figure 18 shows both instantaneous and time-averaged pictures for the contact pair. Figure 18a shows the Na^+ ion completely surrounded by five waters and a Cl^- ion in a strong octahedral structure. A plane of the octahedron is roughly perpendicular to the ion separation vector. Parts b and c in Figure 18 show the individual oxygens for the diffusionally averaged structure over 1 ps for each ion. Figure 18d shows the resultant octahedral cage for the Na^+. Time averaging produces more distortion around the Cl^- ion, illustrating the "soft" character of this hydration shell. It is important to note that on average there are 8 waters in the common first hydration shell around the ion pair. If bridging waters which bond the waters of the octahedral plane around the Na^+ to the backside Cl^- waters are included in the first solvation shell definition this number increases to 11. It appears that these bridging molecules are not retained in their positions as strongly as the first-shell waters as indicated by much less peaked distributions for average oxygen positions.

(11) Belch, A. C.; Rice, S. A.; Sceats, M. G. *Chem. Phys. Lett.* **1981**, *77*, 455. Hirata, F.; Rossky, P. J. *J. Chem. Phys.* **1981**, *74*, 6867.

The transition-state structures are presented in Figure 19. The instantaneous picture shows that one could consider a motion of tilting the octahedron around the Na^+ as the ions are separated. This tilting, which accounts for the decreased population in the first shell of Figure 2, allows another water that was previously bridged to the backside Cl^- waters to attempt to penetrate between the Na^+ and the Cl^-. This does not happen at 3.7 Å for steric reasons and a distorted pentagonal structure results around the Na^+. This structure undergoes many attempts at a relaxation which makes the time-averaged structures in parts b and c of Figure 19 more difficult to define. It is clear, however, that no octahedral structure remains about the Na^+ and no clear structural preference is found about the Cl^-.

The situation at 5.0 Å shows that the water has relaxed into a shared cage with a solvent separating the ions. One easily defines an octahedral structure about the Na^+ in the instantaneous picture in Figure 20a. Figure 20d shows the diffusionally averaged picture with a severely distorted octahedron. The structure around the Cl^- can be compared to an open umbrella with secondary bridging via molecules in region 6.

As the ions separated to 5.6 Å one still obtains a single solvent separated pair, but the octahedron is better defined and the umbrella closes, reducing the participation of second-shell bridging in determining the first-shell structure. Figure 21a shows this effect. Figure 21d shows a better defined time-averaged octahedral structure.

IV. Concluding Remarks

Two structural parameters are important to the dynamics of ion pair separation. First is the need for the Na^+ to maintain octahedral structure in its first hydration sphere. If this cannot be accomplished, the structure of water is disrupted in the second hydration sphere. The pictoral evidence, the hydrogen-bonding distributions, and the dipole angular distributions confirm this structural necessity. Secondly, the chloride must be able to maintain waters about it so that bridge bonding with the FEHS of Na^+ is achieved. This structural feature may be a source of confusion in defining the solvation and coordination number about the ion pairs in solution. These combined structural features suggest that for an ion pair at infinite dilution, it is appropriate to discuss a common cage effect for lifetimes on the order of 1 ps.

The next step in the study will be determining the link between structure and dynamics. This link will help determine the driving force which allows an ion pair to separate, first to the solvent-separated pair and then into solution.

Acknowledgment. The authors thank Prof. Peter Rossky and Dr. Omar Karim for helpful discussions in the early part of this work and thank Prof. William Jorgensen for advice on potential functions. Acknowledgment for partial support is made to the donors of the Petroleum Research Fund, administered by the American Chemical Society (M.B.), the Robert A. Welch Foundation, and NSF (Houston). J.A.M. is an Alfred P. Sloan Fellow and is the recipient of NIH Research Career Development and Camille and Henry Dreyfus Teacher-Scholar Awards.

Registry No. NaCl, 7647-14-5.